Angular distributions of secondary electrons in fast particle-atom scattering

M. Ya. Amusia,[1,2] L. V. Chernysheva,[2] and E. Z. Liverts[1]
[1]*Racah Institute of Physics, The Hebrew University, Jerusalem 91904, Israel*
[2]*Ioffe Physical-Technical Institute, St. Petersburg 194021, Russia*
(Received 19 October 2011; revised manuscript received 18 February 2012; published 30 April 2012)

We present the angular distribution of electrons knocked out from an atom in a fast charge particle collision at small momentum transfer. Not only dipole, but also quadrupole transitions determine this distribution. The contribution of these transitions can be considerably enhanced as compared to the case of photoionization. In photoionization angular distribution, the nondipole parameters are suppressed, as compared to the dipole ones, by the factor $\omega R/c \ll 1$, where ω is the photon energy, R is the ionized shell radius, and c is the speed of light. In fast electron-atom collisions this suppression can be considerably reduced, since the corresponding expansion parameter $\omega R/v \ll 1$ is much bigger than in photoionization, because the speed of the incoming electron $v$is much smaller than c. In formation of the angular distribution, it is decisively important that the ionizing field in the collision process is longitudinal, while in photoionization—it is transversal. We demonstrate that contrary to the case of cross sections, the angular anisotropy parameters for secondary electrons in fast charge particle-atom collisions and in photoionization are essentially different. We illustrate the general formulas by concrete results for outer s, p, and some nd subshells of multielectron noble gas atoms Ar, Kr, and Xe, at several transferred momentum values: $q = 0.0$, 0.1, 1.1, and 2.1. Even for very small transferred momentum q, i.e., in the so-called optical limit, the deviations from the photoionization case are prominent.

DOI: 10.1103/PhysRevA.85.042722 PACS number(s): 34.80.Dp, 31.10.+z, 31.15.V−, 32.80.Fb

I. INTRODUCTION

About 10–15 years ago, a lot of attention was given to the investigation of the so-called nondipole parameters of photoelectron angular distributions (see Refs. [1–3], and references therein). It was understood that this is in fact the only way to reveal the contribution of quadrupole continuous spectrum matrix elements of atomic electrons, which in the absolute photoionization cross section are unobservable in the shadow of much bigger dipole contributions. To study nondipole parameters, the high intensity sources of continuous spectrum electromagnetic radiation were used [4–7].

By the order of magnitude, the ratio of quadrupole-to-dipole matrix elements in photoionization is characterized by the parameter $\omega R/c$, where ω is the photon energy, R is the ionized shell radius, and c is the speed of light. For photon energies up to several keV, which includes the ionization potential of the inner $1s$ subshell even for medium atoms, one has $\omega R/c \ll 1$. In the absolute cross sections, the dipole and quadrupole terms do not interfere, so that the second power of the small parameter $\omega R/c$ determines the ratio of quadrupole-to-dipole contributions. In addition, some of these terms cancel each other. As to the angular distribution, it includes the dipole-quadrupole interference terms that are in the first power of $\omega R/c$, and therefore the relative role of quadrupole terms is much bigger.

Quite long ago the fast charged particle inelastic scattering process was considered as a "synchrotron for the poor" [8]. This notion reflects the fact that the fast charge particle inelastic scattering is similar to photoionization, since the dipole contribution mainly determines it. However, contrary to the photoionization case, the ratio "quadrupole-to-dipole" contributions can be much bigger, since instead of $\omega R/c$, the parameter $\omega R/\upsilon$, where υ is the speed of the projectile, determines it. Because $1 \ll \upsilon \ll c$, the role of the quadrupole term in inelastic scattering is relatively much bigger.[1]

The momentum q transferred in the collision is not bound to the transferred energy ω by a relation $\omega = aq$, with a being a constant, similar to the case of photoionization, with $\omega = cq$. Therefore, the collision experiment gives an extra degree of freedom to control the atomic reaction to the transferred energy and linear momentum. This stimulates the current research. Its aim is to derive formulas for the angular anisotropy parameters of electrons emitted off an atom in its inelastic scattering with a fast charged projectile. We also perform calculations of these parameters as functions of ω and q. Note that the information from the photoionization studies does not inform one at all about the q dependences of dipole and quadrupole matrix elements or about the monopole matrix elements. As far as we know, the angular anisotropy parameters presented in this paper are derived for the first time.

Here we suggest investigation of the cross section of the inelastic scattering on an atom and the study of the angular distribution of the emitted electrons relative to the momentum q transferred to the atom from the projectile. As is well known, the fast charged particle inelastic scattering cross section is proportional to the so-called generalized oscillator strength (GOS) density. Therefore, in this paper we study the GOS density angular distribution as a function of the angle θ between the momentum of the electron emitted in the collision process and of direction $\vec{q}$.

Deep similarity between the photoionization and the fast electron scattering brought to belief that not only the total cross section, but also the angular anisotropy parameters are

[1]The atomic system of units is used in this paper: electron charge e, its mass m, and Planck constant $\hbar$ being equal to 1, $e = m = \hbar = 1$.

either the same or similar. As we show below, this is incorrect even in the so-called optical limit $q \to 0$.

In our calculations, we will not limit ourselves to the one-electron Hartree-Fock approximation, but will also include multielectron correlations in the frame of the random phase approximation with exchange (RPAE) that was successfully applied to studies of photoionization and fast electron scattering [9,10]. We published formulas and some data for s subshells in Ref. [11]. Here we present some more calculation data for s subshells and new results, both analytic and numeric, for p and d subshells.

Overall, what is done in this paper is the further development of the idea of the "synchrotron for the pure" [8] in the investigation of atoms along the same direction, in which one can use normal synchrotron radiation. We demonstrate some of the advantages of fast electron scattering that already opens up the possibility to study not only dipole but also monopole and quadrupole transitions (see Refs. [12,13], and references therein).[2]

Let us compare our approach to that developed in connection to the studies of the so-called $(e,2e)$ reaction [14–17]. In most cases, the electrons were not fast enough and the first Born approximation in describing the incoming electrons was not valid. The angle of the geometry used was obviously different from that used in this paper. The aim of this direction of research was clearly formulated in Ref. [17]: "A specific set of kinematics is completely defined by the method with the results yielding valuable information on the collision dynamics or on the momentum distribution of the struck atomic electron." It required developing approaches that permitted one to take into account the interaction between two outgoing electrons.

In this paper, the aims and approach are different. We suggest using fast incoming electrons as a source of transferred to the atom energy ω and momentum q. This means that we consider so high incoming energies that their interaction with the target is sufficient to treat in the first Born approximation. For medium heavy atoms, it corresponds to tens of keV.

Our aim here is to study the reaction of a target atom to the absorption of ω and q at small q. This is why the suggested geometry of experiment, the method of results description, etc., are entirely different from those used in $(e,2e)$ studies.

In our approach, we determine the angular distribution of the investigated electron by several parameters that are dependent upon ω and q, and independent upon the electron emission angle θ. We present analytic expressions for these parameters along with their numeric values obtained in the frame of RPAE. In spite of extensive investigation of the fast electron scattering, there are no experiments suggested in this paper on fast electron energy and collision geometry. In this sense, the present research is a call to experimentalists to perform the required measurements.

[2]The decisive contribution of the monopole GOS component in Ar $3p$-$4p$ transition was predicted in Ref. [12] and later confirmed in Ref. [13]. Thus, this part of the $3p$-$4p$ transition is not seen in photoabsorption at all.

II. MAIN FORMULAS

Here for completeness we start with the well-known expressions. Some formulas for s- subshell angular anisotropy parameters we have already presented in Ref. [11]. We repeat them here for completeness and the convenience of the reader.

The cross section of the fast electron inelastic scattering upon an atom with ionization of an electron of nl subshell can be presented [18,19] as follows:

$$\frac{d^2\sigma_{nl}}{d\omega\, dq} = \frac{2\sqrt{(E-\omega)}}{\sqrt{E}\omega q^2}\frac{dF_{nl}(q,\omega)}{d\omega}. \tag{1}$$

Here $dF_{nl}(q,\omega)/d\omega$ is the GOS density differential in the ionized electron energy $\varepsilon = \omega - I_{nl}$, where I_{nl} is the nl subshell ionization potential.

The following formula gives, in one-electron approximation, the GOS density differential both in the emission angle and in the energy of the ionized electron with linear momentum $\vec{k}$ from a subshell with principal quantum number n and angular momentum l:

$$\frac{df_{nl}(q,\omega)}{d\Omega} = \frac{1}{2l+1}\frac{2\omega}{q^2}\sum_m |\langle nlms|\exp(i\vec{q}\cdot\vec{r})|\varepsilon\vec{k}s\rangle|^2. \tag{2}$$

Here $\vec{q} = \vec{p} - \vec{p}'$, with $\vec{p}$ and $\vec{p}'$ being the linear moments of the fast incoming and outgoing electrons determined by the initial E and final E' energies as $p = \sqrt{2E}$ and $p' = \sqrt{2E'}$, Ω is the solid angle of the emitted electron, m is the angular momentum projection, and s is the electron spin. Note that $\omega = E - E'$, $\omega = p^2/2 - (\vec{p}-\vec{q})^2/2 = \vec{p}\cdot\vec{q} - q^2/2$, and $\varepsilon = \omega - I_{nl}$ is the outgoing electron energy.

The values of ω are limited by the relation $0 \leqslant \omega \leqslant pq - q^2/2$, contrary to the proportionality $\omega = cq$ for the case of photoeffect. In order to consider the projectile as fast, its speed must be much higher than the speed of electrons in the ionized subshell, i.e., $\sqrt{2E} \gg R^{-1}$. The transferred-to-the-atom momentum q is small if $qR \leqslant 1$.

Expanding $\exp(i\vec{q}\cdot\vec{r})$ into a sum of products of radial and angular parts and performing analytic integration over the angular variables, one obtains for GOS in the one-electron Hartree-Fock approximation,

$$g_{nl,kl',L}(q) \equiv \int_0^\infty R_{nl}(r) j_L(qr) R_{kl'}(r) r^2\, dr, \tag{3}$$

where $j_L(qr)$ are the spherical Bessel functions and $R_{nl(kl')}(r)$ are the radial parts of the Hartree-Fock (HF) electron wave functions in the initial (final) states.

We suggest measuring the angular distribution of the emitted electrons relative to the direction of $\vec{q}$. This means that the z axis coincides with the direction of $\vec{q}$ and hence one has to put $\theta_{\vec{q}} = \varphi_{\vec{q}} = 0$ in Eq. (2). Since we have in mind ionization of the particular nl subshell, for simplicity of notation let us introduce the following abbreviations: $g_{nl,kl',L}(q) \equiv g_{kl'L}(q)$. Note that due to energy conservation in the fast electron inelastic scattering process one has $k = \sqrt{2(\omega - I_{nl})}$.

We can generalize the GOS formulas in order to include the interelectron correlations in the frame of RPAE. We achieve this by substituting $g_{kl'L'}(q)$ with modulus $\tilde{G}_{kl'L'}(q)$ and the scattering phases $\delta_{l'}$ with $\bar{\delta}_{l'} = \delta_{l'} + \Delta_{l'}$, where the expressions $G_{kl'L'}(q) \equiv \tilde{G}_{kl'L'}(q)\exp(i\Delta_{l'})$ are solutions of the RPAE set

of equations [20]:

$$\langle \varepsilon l'|G^L(\omega,q)|nl\rangle = \langle \varepsilon l'|j_L(qr)|nl\rangle + \left(\sum_{\varepsilon''l''\leqslant F,\varepsilon'''l'''>F} - \sum_{\varepsilon''l''<F,\varepsilon'''l'''\leqslant F}\right) \frac{\langle \varepsilon'''l'''|G^L(\omega,q)|\varepsilon''l''\rangle\langle \varepsilon''l'',\varepsilon l'|U|\varepsilon'''l''',nl\rangle_L}{\omega - \varepsilon_{\varepsilon'''l'''} + \varepsilon_{\varepsilon''l''} + i\eta(1-2n_{\varepsilon'''l'''})}. \quad (4)$$

Here $\leqslant F$ ($>F$) denotes the summation over occupied (vacant) atomic levels in the target atom. Summation over vacant levels includes integration over continuous spectrum; $n_{\varepsilon l}$ is the Fermi step function that is equal to 1 for $nl \leqslant F$ and 0 for $nl > F$; the Coulomb interelectron interaction matrix element is defined as $\langle \varepsilon''l'',\varepsilon l'|U|\varepsilon'''l''',nl\rangle_L = \langle \varepsilon''l'',\varepsilon l'|r_<^L/r_>^{L+1}|\varepsilon'''l''',nl\rangle - \langle \varepsilon''l'',\varepsilon l'|r_<^L/r_>^{L+1}|nl,\varepsilon'''l'''\rangle$ and $\eta \to +0$. In the latter formula, the notation of smaller (bigger) radiuses of $r_<$ ($r_>$) of interacting electron coordinates comes from the well-known expansion of the Coulomb interelectron interaction. The necessary details about solving (4) one can find in Ref. [21].

For differentials in the outgoing electron angle GOS density of nl subshell $dF_{nl}(q,\omega)/d\Omega$, the following relations are valid in RPAE [10]:

$$\begin{aligned}\frac{dF_{nl}(q,\omega)}{d\Omega} &= \sum_{L'L''}\frac{dF_{nl}^{L',L''}(q,\omega)}{d\Omega} = \frac{\omega\pi}{q^2}\sum_{L'L''}(2L'+1)(2L''+1)i^{L'-L''} \\ &\times \sum_{l'=|L'-l|}^{L'+l}\sum_{l''=|L''-l|}^{L''+l}\tilde{G}_{kl'L'}(q)\tilde{G}_{kl''L''}(q)i^{l''-l'}(2l'+1)(2l''+1)e^{i(\bar{\delta}_{l'}-\bar{\delta}_{l''})}\begin{pmatrix} L' & l & l' \\ 0 & 0 & 0\end{pmatrix}\begin{pmatrix} l'' & l & L'' \\ 0 & 0 & 0\end{pmatrix} \\ &\times \sum_{L=|l'-l''|}^{l'+l''}P_L(\cos\theta)(-1)^{L+l}(2L+1)\begin{pmatrix} l' & L & l'' \\ 0 & 0 & 0\end{pmatrix}\begin{pmatrix} L & L' & L'' \\ 0 & 0 & 0\end{pmatrix}\begin{Bmatrix} L & L' & L'' \\ l & l'' & l'\end{Bmatrix}. \quad (5)\end{aligned}$$

This expression follows by generalizing (2) to include the RPAE corrections and performing required analytical integrations and summations over projection of the electron angular moments m with the help of the MATHEMATICA package [22].

From (5), the partial value of GOS $F_{nl}(q,\omega)$ in RPAE can be obtained by integrating over $d\Omega$, leading to the following expressions:

$$F_{nl}(q,\omega) = \sum_{L'}F_{nl}^{L'}(q,\omega) = \frac{4\omega\pi^2}{q^2}\sum_{L'}(2L'+1)\sum_{l'=|L'-l|}^{L'+l}[\tilde{G}_{kl'L'}(q)]^2(2l'+1)\begin{pmatrix} L' & l & l' \\ 0 & 0 & 0\end{pmatrix}^2. \quad (6)$$

Note that at small q the dipole contribution in GOSs $F_{nl}(q,\omega)$ dominates and is simply proportional to the photoionization cross section $\sigma_{nl}(\omega)$ [10]. To compare the results obtained with known formulas for the photoionization with lowest-order nondipole corrections taken into account, let us consider so small q that it is enough to take into account terms with $L',L'' \leqslant 2$. In this case, we can present the GOS angular distribution (5) in a way that is similar to the photoionization case, as

$$\frac{dF_{nl}(q,\omega)}{d\Omega} = \frac{F_{nl}(q,\omega)}{4\pi}\left\{1 - \frac{\beta_{nl}^{(\mathrm{in})}(\omega,q)}{2}P_2(\cos\theta) + q\left[\gamma_{nl}^{(\mathrm{in})}(\omega,q)P_1(\cos\theta) + \eta_{nl}^{(\mathrm{in})}(\omega,q)P_3(\cos\theta) + \varsigma_{nl}^{(\mathrm{in})}(\omega,q)P_4(\cos\theta)\right]\right\}. \quad (7)$$

The obvious difference is the presence of q dependence of the coefficients and an extra term $\varsigma_{nl}^{(\mathrm{in})}(\omega,q)P_4(\cos\theta)$. Even in this case of $L',L'' \leqslant 2$, expressions for $\beta_{nl}^{(\mathrm{in})}(\omega,q)$, $\gamma_{nl}^{(\mathrm{in})}(\omega,q)$, $\eta_{nl}^{(\mathrm{in})}(\omega,q)$, and $\varsigma_{nl}^{(\mathrm{in})}(\omega,q)$ via $g_{kl'L'}(q)$ are too complex as compared to relations for $\beta_{nl}(\omega)$, $\gamma_{nl}(\omega)$, and $\eta_{nl}(\omega)$ in photoionization. Therefore, it is more convenient to present the results for s, p, and d subshells separately. We demonstrate that while $F_{nl}(q,\omega) \sim \sigma(\omega)$, similar relations are not valid for the anisotropy parameters.

Let us start with s subshells, where, as follows from (5), the following relation gives differential GOSs in the above-mentioned $L',L'' \leqslant 2$ approximation:

$$\begin{aligned}\frac{dF_{ns}(q,\omega)}{d\Omega} &= \sum_{L',L''=0}^{2}\frac{dF_{ns}^{L',L''}(q,\omega)}{d\Omega} = \frac{F_{ns}(q,\omega)}{4\pi}\left\{1 + \frac{6}{W_0}\tilde{G}_{11}[\tilde{G}_{00}\cos(\bar{\delta}_0-\bar{\delta}_1) + 2\tilde{G}_{22}\cos(\bar{\delta}_1-\bar{\delta}_2)]P_1(\cos\theta)\right. \\ &+ \frac{2}{7W_0}\left\{21\tilde{G}_{11}^2 + 5\tilde{G}_{22}[7\tilde{G}_{00}\cos(\bar{\delta}_0-\bar{\delta}_2) + 5\tilde{G}_{22}]\right\}P_2(\cos\theta) \\ &\left. + \frac{18}{W_0}\tilde{G}_{11}\tilde{G}_{22}\cos(\bar{\delta}_1-\bar{\delta}_2)P_3(\cos\theta) + \frac{90}{7W_0}\tilde{G}_{22}^2P_4(\cos\theta)\right\} \\ &\equiv \frac{F_{ns}(q,\omega)}{4\pi}\left\{1 - \frac{1}{2}\beta_{ns}^{(\mathrm{in})}(q,\omega)P_2(\cos\theta) + q\left[\gamma_{ns}^{(\mathrm{in})}(q,\omega)P_1(\cos\theta) + \eta_{ns}^{(\mathrm{in})}(q,\omega)P_3(\cos\theta)\right]\right\}, \quad (8)\end{aligned}$$

where

$$F_{ns} = \frac{4\pi^2\omega}{q^2}W_0; \quad W_0 = \tilde{G}_{00}^2 + 3\tilde{G}_{11}^2 + 5\tilde{G}_{22}^2. \quad (9)$$

We will compare the result obtained in the small q limit with the known formula for photoionization of an atom by nonpolarized light [1]. To do this, we have to use the lowest-order terms of the first four spherical Bessel functions:

$$j_0(qr) \cong 1 - \frac{(qr)^2}{6}; \quad j_1(qr) \cong \frac{qr}{3}\left(1 - \frac{(qr)^2}{10}\right);$$
$$j_2(qr) \cong \frac{(qr)^2}{15}\left(1 - \frac{(qr)^2}{14}\right); \quad j_3(qr) \cong \frac{(qr)^3}{105}. \tag{10}$$

The lowest in the powers of q term is $\tilde{G}_{11} \sim q \ll 1$.[3] The correction to $\tilde{G}_{11}$ is proportional to q^3. As to $\tilde{G}_{00}$ and $\tilde{G}_{22}$, they are proportional to q^2 with corrections of the order ofq^4. By retaining in Eq. (8) terms of the order of q^2 and greater, one obtains the following expression:

$$\frac{dF_{ns}(q,\omega)}{d\Omega} = \frac{F_{ns}(q,\omega)}{4\pi}\left\{1 + 2P_2(\cos\theta) + \frac{2}{\tilde{G}_{11}}[\tilde{G}_{00}\cos(\bar{\delta}_0 - \bar{\delta}_1) + 2\tilde{G}_{22}\cos(\bar{\delta}_1 - \bar{\delta}_2)]P_1(\cos\theta) + \frac{6\tilde{G}_{22}}{\tilde{G}_{11}}\cos(\bar{\delta}_1 - \bar{\delta}_2)P_3(\cos\theta)\right\}$$
$$\equiv \frac{F_{ns}(q,\omega)}{4\pi}\left\{1 + 2P_2(\cos\theta) + q\left[\gamma_{ns}^{(\mathrm{in})}(q,\omega)P_1(\cos\theta) + \eta_{ns}^{(\mathrm{in})}(q,\omega)P_3(\cos\theta)\right]\right\}. \tag{11}$$

One should compare this relation with the similar one for photoionization of the ns subshell [1]:

$$\frac{d\sigma_{ns}(\omega)}{d\Omega} = \frac{\sigma_{ns}(\omega)}{4\pi}\left\{1 - P_2(\cos\theta) + \kappa\frac{6\tilde{Q}_2}{5\tilde{D}_1}\cos(\bar{\delta}_1 - \bar{\delta}_2)[P_1(\cos\theta) - P_3(\cos\theta)]\right\}$$
$$\equiv \frac{\sigma_{ns}(\omega)}{4\pi}\{1 - P_2(\cos\theta) + \kappa[\gamma_{ns}(\omega)P_1(\cos\theta) + \eta_{ns}(\omega)P_3(\cos\theta)]\}. \tag{12}$$

where $\kappa = \omega/c$ is the photon momentum, and $\gamma_{ns}(\omega) = -\eta_{ns}(\omega) = (6\tilde{Q}_2/5\tilde{D}_1)\cos(\bar{\delta}_1 - \bar{\delta}_2)$.

The sign and magnitude of the dipole parameter is different for inelastic fast electron scattering, as follows from the comparison of (11) and (12). This parameter in the electron scattering is two times bigger than in the photoionization and of opposite sign. Essentially different are the expressions for the nondipole terms. This difference exists and remains even in the so-called optical limit $q \to 0$.

According to Eq. (10), in the $q \to 0$ limit there are simple relations between dipole $\tilde{D}_1$ and quadrupole $\tilde{Q}_2$ matrix elements and functions $\tilde{G}_{11}$,$\tilde{G}_{22}$, namely, $\tilde{G}_{11} = q\tilde{D}_1/3$ and $\tilde{G}_{22} = 2q^2\tilde{Q}_2/15$. With the help of these relations and $\tilde{G}_{00} = -q^2\tilde{Q}_2/3 = -(5/2)\tilde{G}_{22}$, formula (11) transforms into the following expression:

$$\frac{dF_{ns}(q,\omega)}{d\Omega} = \frac{F_{ns}(q,\omega)}{4\pi}\left\{1 + 2P_2(\cos\theta) + q\left[\frac{2\tilde{Q}_2}{\tilde{D}_1}\left(\frac{4}{5}\cos(\bar{\delta}_1 - \bar{\delta}_2) - \cos(\bar{\delta}_0 - \bar{\delta}_1)\right) \times P_1(\cos\theta) + 2\gamma_{ns}(\omega)P_3(\cos\theta)\right]\right\}. \tag{13}$$

The deviation from (12) is evident, since one cannot express the angular distribution in inelastic scattering via a single nondipole parameter $\gamma_{ns}(\omega)$ including the absent in photoionization phase difference $\bar{\delta}_0 - \bar{\delta}_1$. As a result, the following relations have to be valid at very small q:

$$\gamma_{ns}^{(\mathrm{in})}(\omega) = \frac{2\tilde{Q}_2}{\tilde{D}_1}\left[\frac{4}{5}\cos(\bar{\delta}_1 - \bar{\delta}_2) - \cos(\bar{\delta}_0 - \bar{\delta}_1)\right],$$
$$\eta_{ns}^{(\mathrm{in})}(\omega) = 2\gamma_{ns}(\omega) = \frac{12}{5}\frac{\tilde{Q}_2}{\tilde{D}_1}\cos(\bar{\delta}_1 - \bar{\delta}_2). \tag{14}$$

We see that the investigation of inelastic scattering even at $q \to 0$ permits one to obtain an additional characteristic of the ionization process, namely, its s-wave phase.

It will be demonstrated below that for $l > 0$, even at very small q, the relations between nondipole parameters in the photoionization and the inelastic fast electron scattering are more complex.

The similarity of general structure and considerable difference between (11) and (12) is evident. Indeed, one can enhance the contribution of the nondipole parameters, since the condition $\omega/c \ll q \ll R^{-1}$ is easy to achieve. Let us note that even while neglecting the terms with q, (12) and (13) remain different: in photoionization, the angular distribution is proportional to $\sin^2\theta$ [see Eq. (12)], whereas in the inelastic scattering it is proportional to $\cos^2\theta$ [see Eq. (13)]. The reason for this difference is clear. In photoabsorption, the atomic electron is "pushed" off the atom by the electric field of the photon, which is perpendicular to the direction of the light beam. In inelastic scattering, the "push" acts along momentum $\vec{q}$, so the preferential emission of the electrons takes place along the $\vec{q}$ direction, so the maximum is at $\theta = 0$. Similar reason explains the difference in the nondipole terms. Note that the last term due to monopole transition in Eq. (13) is absent in photoabsorption angular distribution (12). It confirms that the angular distribution of the GOS densities is richer than that of photoionization.

[3]As is seen from (10), we have in mind such values of q that $qR < 1$.

Although the expressions for p and d subshells are much more complex than that for s, they are of great importance and interest since p and d subshells are multielectron objects. As such, the intrashell electron correlations may affect them. Particularly important are the multielectron effects in the $4d$ subshell due to the presence there of the famous dipole giant resonance (see, e.g., [10]). This is why it is of interest to present data on non-s subshells also.

While in Ref. [11] we have obtained formulas for s subshells only, here we present data for differential GOSs of p and d' subshells. For p' subshells ($l = 1$) the following expression is obtained:

$$
\begin{aligned}
&\frac{dF_{np}(q,\omega)}{d\Omega} \\
&= \sum_{L',L''=0}^{2} \frac{dF_{np}^{L',L''}(q,\omega)}{d\Omega} \\
&= \frac{F_{np}}{4\pi}\Bigg(1 + \frac{1}{5W_1}\{10\tilde{G}_{01}(2\tilde{G}_{12} - \tilde{G}_{10})\cos(\bar{\delta}_0 - \bar{\delta}_1) + 4\tilde{G}_{21}[(5\tilde{G}_{10} - \tilde{G}_{12})\cos(\bar{\delta}_1 - \bar{\delta}_2) + 9\bar{G}_{32}\cos(\bar{\delta}_2 - \bar{\delta}_3)]\}P_1(\cos\theta) \\
&\quad + \frac{2}{7W_1}\{7\tilde{G}_{21}[\tilde{G}_{21} - 2\tilde{G}_{01}\cos(\bar{\delta}_0 - \bar{\delta}_2)] + 7\tilde{G}_{12}(\tilde{G}_{12} - 2\tilde{G}_{10}) + 3\tilde{G}_{32}[(7\tilde{G}_{10} - 2\tilde{G}_{12})\cos(\bar{\delta}_1 - \bar{\delta}_3) + 4\tilde{G}_{32}]\}P_2(\cos\theta) \\
&\quad - \frac{6}{5W_1}\{6\tilde{G}_{21}\tilde{G}_{12}\cos(\bar{\delta}_1 - \bar{\delta}_2) + \tilde{G}_{32}[5\tilde{G}_{01}\cos(\bar{\delta}_0 - \bar{\delta}_3) - 4\tilde{G}_{21}\cos(\bar{\delta}_2 - \bar{\delta}_3)]\}P_3(\cos\theta) \\
&\quad + \frac{18}{7W_1}\tilde{G}_{32}[\tilde{G}_{32} - 4\tilde{G}_{12}\cos(\bar{\delta}_1 - \bar{\delta}_3)]P_4(\cos\theta)\Bigg) \\
&\equiv \frac{F_{np}(q,\omega)}{4\pi}\left\{1 - \frac{\beta_{np}^{(\mathrm{in})}(q,\omega)}{2}P_2(\cos\theta) + q[\gamma_{np}^{(\mathrm{in})}(q,\omega)P_1(\cos\theta) + \eta_{np}^{(\mathrm{in})}(q,\omega)P_3(\cos\theta) + \zeta_{np}^{(\mathrm{in})}(q,\omega)P_4(\cos\theta)]\right\},
\end{aligned}
\tag{15}
$$

where

$$
F_{np} = \frac{4\pi^2\omega}{q^2}W_1; \quad W_1 = \tilde{G}_{10}^2 + \tilde{G}_{01}^2 + 2\left[\tilde{G}_{21}^2 + \tilde{G}_{12}^2\right] + 3\tilde{G}_{32}^2. \tag{16}
$$

For differential GOSs of d subshells ($l = 2$) the following expression holds:

$$
\begin{aligned}
\frac{dF_{nd}(q,\omega)}{d\Omega} &= \frac{F_{nd}}{4\pi}\Bigg(1 + \frac{6}{W_2}\{14\tilde{G}_{11}(\tilde{G}_{22} - \tilde{G}_{20})\cos(\bar{\delta}_1 - \bar{\delta}_2) - 14\tilde{G}_{11}\tilde{G}_{02}\cos(\bar{\delta}_0 - \bar{\delta}_1) \\
&\quad + 3\tilde{G}_{31}[(7\tilde{G}_{20} - 2\tilde{G}_{22})\cos(\bar{\delta}_2 - \bar{\delta}_3) + 12\tilde{G}_{42}\cos(\bar{\delta}_3 - \bar{\delta}_4)]\}P_1(\cos\theta) \\
&\quad + \frac{2}{245W_2}\left\{1029\left(\tilde{G}_{11}^2 + 6\tilde{G}_{31}^2\right) - 18522\tilde{G}_{11}\tilde{G}_{31}\cos(\bar{\delta}_1 - \bar{\delta}_3) + 1225\tilde{G}_{02}(7\tilde{G}_{20} - 10\tilde{G}_{22})\cos(\bar{\delta}_0 - \bar{\delta}_2)\right. \\
&\quad \left. - 125\tilde{G}_{22}(98\tilde{G}_{20} + 15\tilde{G}_{22}) + 450\tilde{G}_{42}[(49\tilde{G}_{20} - 20\tilde{G}_{22})\cos(\bar{\delta}_2 - \bar{\delta}_4) + 25\tilde{G}_{42}]\right\}P_2(\cos\theta) \\
&\quad + \frac{18}{W_2}[2\tilde{G}_{11}[\tilde{G}_{22}\cos(\bar{\delta}_1 - \bar{\delta}_2) - 6\tilde{G}_{42}\cos(\bar{\delta}_1 - \bar{\delta}_4)] + \tilde{G}_{31}[7\tilde{G}_{02}\cos(\bar{\delta}_0 - \bar{\delta}_3) \\
&\quad - 8\tilde{G}_{22}\cos(\bar{\delta}_2 - \bar{\delta}_3) + 6\tilde{G}_{42}\cos(\bar{\delta}_3 - \bar{\delta}_4)]P_3(\cos\theta) \\
&\quad + \frac{90}{49W_2}\left\{20\tilde{G}_{22}^2 + \tilde{G}_{42}[98\tilde{G}_{02}\cos(\bar{\delta}_0 - \bar{\delta}_4) - 100\tilde{G}_{22}\cos(\bar{\delta}_2 - \bar{\delta}_4) + 27\tilde{G}_{42}]\right\}P_4(\cos\theta)\Bigg) \\
&\equiv \frac{F_{nd}(q,\omega)}{4\pi}\left\{1 - \frac{\beta_{nd}^{(\mathrm{in})}(q,\omega)}{2}P_2(\cos\theta) + q\left[\gamma_{nd}^{(\mathrm{in})}(q,\omega)P_1(\cos\theta) + \eta_{nd}^{(\mathrm{in})}(q,\omega)P_3(\cos\theta) + \zeta_{nd}^{(\mathrm{in})}(q,\omega)P_4(\cos\theta)\right]\right\},
\end{aligned}
\tag{17}
$$

where

$$
F_{nd} = \frac{4\pi^2\omega}{35q^2}W_2; \qquad W_2 = 35\tilde{G}_{20}^2 + 42\tilde{G}_{11}^2 + 63\tilde{G}_{31}^2 + 35\tilde{G}_{02}^2 + 50\tilde{G}_{22}^2 + 90\tilde{G}_{42}^2. \tag{18}
$$

It is interesting to compare, just as was done with $l = 0$, the expressions (15) and (17) with the angular distribution of photoelectrons. It is essential to clarify whether the difference exists even in the $q \to 0$ limit, as takes place for the s subshells. In this limit, the following expressions follow from (15) and (17):

For $l = 1$ one has from (15) at $q = 0$,

$$
\beta_{np}^{(\mathrm{in})}(q = 0,\omega) = -\frac{4}{\tilde{D}_0^2 + 2\tilde{D}_2^2}\left[\tilde{D}_2^2 - 2\tilde{D}_0\tilde{D}_2\cos(\bar{\delta}_0 - \bar{\delta}_2)\right], \tag{19}
$$

$$\gamma_{np}^{(\mathrm{in})}(q=0,\omega)=\frac{18}{25\left[\tilde{D}_0^2+2\tilde{D}_2^2\right]}\{5\tilde{D}_0\tilde{Q}_1\cos(\bar{\delta}_1-\bar{\delta}_0)+2\tilde{D}_2[2\tilde{Q}_3\cos(\bar{\delta}_3-\bar{\delta}_2)-3\tilde{Q}_1\cos(\bar{\delta}_1-\bar{\delta}_2)]\}, \tag{20}$$

$$\eta_{np}^{(\mathrm{in})}(q=0,\omega)=\frac{12}{25\left[\tilde{D}_0^2+2\tilde{D}_2^2\right]}\{5\tilde{D}_0\tilde{Q}_3\cos(\bar{\delta}_3-\bar{\delta}_0)+2\tilde{D}_2[3\tilde{Q}_1\cos(\bar{\delta}_1-\bar{\delta}_2)-2\tilde{Q}_3\cos(\bar{\delta}_3-\bar{\delta}_2)]\}. \tag{21}$$

For $l=2$ one has from (17) at $q=0$,

$$\beta_{nd}^{(\mathrm{in})}(q=0,\omega)=-\frac{4}{5\left[2\tilde{D}_1^2+3\tilde{D}_3^2\right]}\left[\tilde{D}_1^2+6\tilde{D}_3^2-18\tilde{D}_1\tilde{D}_3\cos(\bar{\delta}_1-\bar{\delta}_3)\right], \tag{22}$$

$$\gamma_{nd}^{(\mathrm{in})}(q=0,\omega)=\frac{2}{35\left[2\tilde{D}_1^2+3\tilde{D}_3^2\right]}\{14\tilde{D}_1[7\tilde{Q}_2\cos(\bar{\delta}_1-\bar{\delta}_2)-2\tilde{Q}_0\cos(\bar{\delta}_0-\bar{\delta}_1)]+9\tilde{D}_3[8\tilde{Q}_4\cos(\bar{\delta}_4-\bar{\delta}_3)-13\tilde{Q}_2\cos(\bar{\delta}_2-\bar{\delta}_3)]\}, \tag{23}$$

$$\eta_{nd}^{(\mathrm{in})}(q=0,\omega)=\frac{12}{35\left[2\tilde{D}_1^2+3\tilde{D}_3^2\right]}\{2\tilde{D}_1[\tilde{Q}_2\cos(\bar{\delta}_2-\bar{\delta}_1)-6\tilde{Q}_4\cos(\bar{\delta}_4-\bar{\delta}_1)]+\tilde{D}_3[7\tilde{Q}_0\cos(\bar{\delta}_0-\bar{\delta}_3)-8\tilde{Q}_2\cos(\bar{\delta}_2-\bar{\delta}_3)-6\tilde{Q}_4\cos(\bar{\delta}_4-\bar{\delta}_3)]\}. \tag{24}$$

In deriving formulas (19)–(24), we use the following relations:

$$\tilde{G}_{l'1}\equiv\frac{q}{3}\tilde{D}_{l'}(l'=l\pm1);\quad \tilde{G}_{l'0}\equiv-\frac{q^2}{3}\tilde{Q}_{l'}(l'=l);\qquad \tilde{G}_{l'2}\equiv\frac{2q^2}{15}\tilde{Q}_{l'}\quad(l'=l,l\pm2). \tag{25}$$

To clarify comparison between the angular anisotropy parameters in photoionization and fast electron scattering, note that we use the following relations in the HF approximation for dipole and quadrupole radial matrix elements

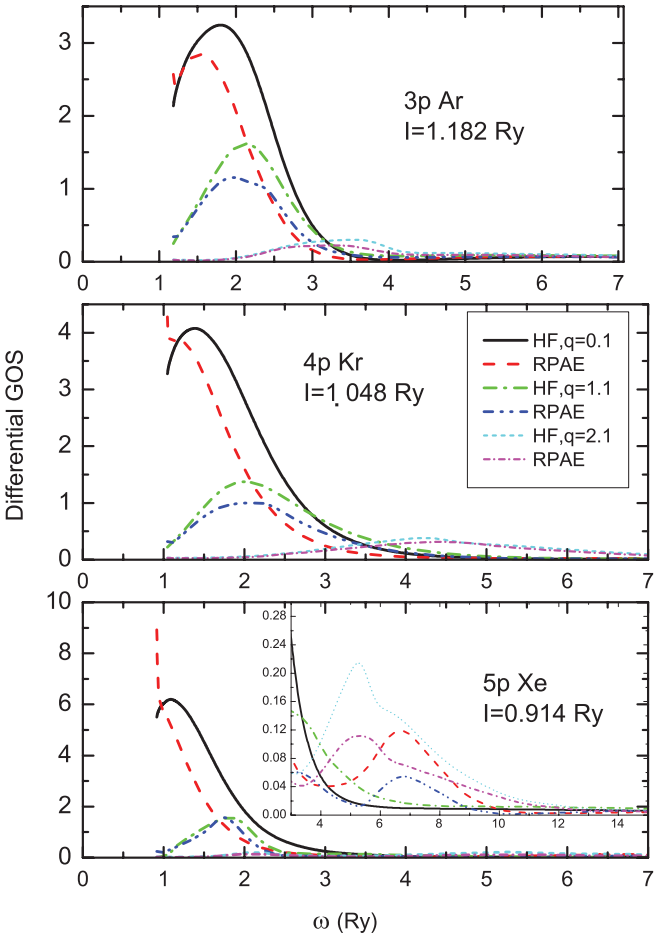

FIG. 1. (Color online) Differential generalized oscillator strength given by (15) at the magic angle $\theta_m\cong54.7^\circ$ of $3p$, $4p$, and $5p$ subshells for Ar, Kr, and Xe at $q=0.1$, 1.1, and 2.1 in HF and RPAE.

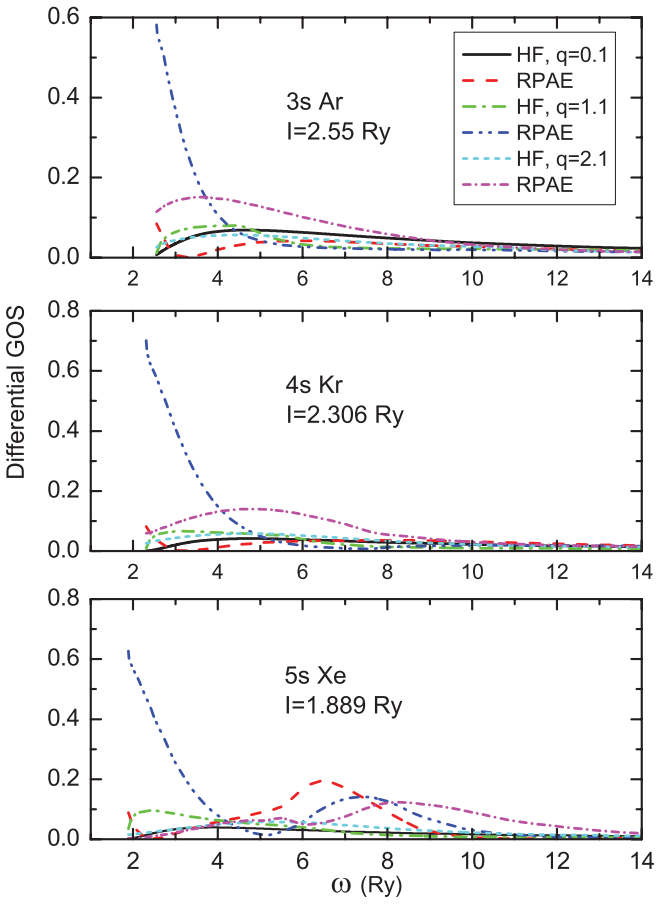

FIG. 2. (Color online) Differential generalized oscillator strength given by (8) at the magic angle $\theta_m\cong54.7^\circ$ of $3s$, $4s$, and $5s$ subshells for Ar, Kr, and Xe at $q=0.1$, 1.1, and 2.1 in HF and RPAE.

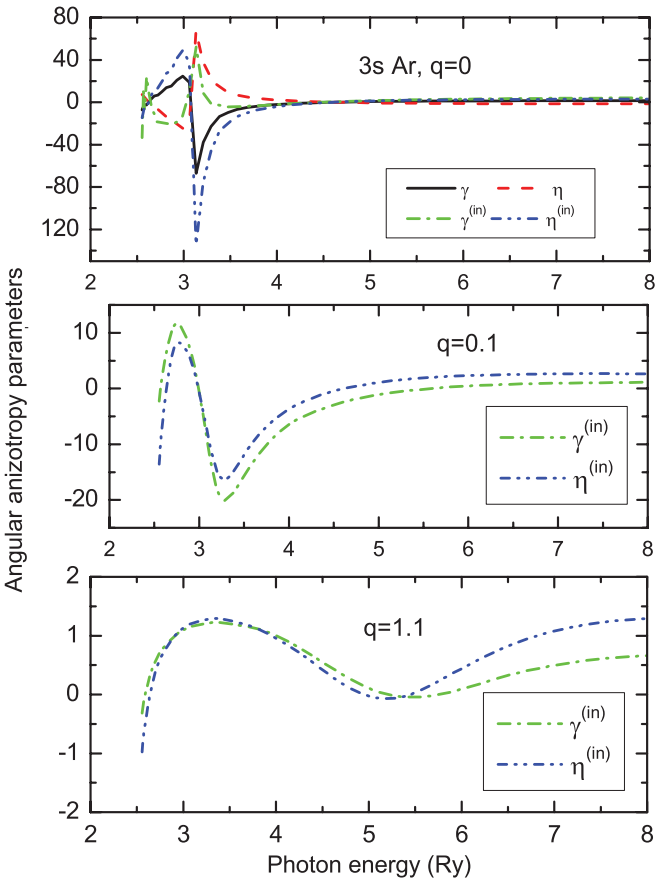

FIG. 3. (Color online) Angular anisotropy nondipole parameters of knocked-out electrons $\gamma_{ns}^{(\mathrm{in})}(\omega)$ and $\eta_{ns}^{(\mathrm{in})}(\omega)$ given by (8) and (13) at $q = 0.01$, 0.1, and 1.1, compared to similar parameters in photoionization $\gamma_{ns}(\omega)$ and $\eta_{ns}(\omega)$ (12) for the $3s$ subshell of Ar in RPAE.

$\tilde{d}_{l'}$ and $\tilde{q}_{l'}$:

$$\begin{aligned} \tilde{D}_{l'} \Rightarrow \tilde{d}_{l'} &= \int_0^\infty P_{nl}(r) r P_{kl'}(r) dr; \\ \tilde{Q}_{l'} \Rightarrow \tilde{q}_{l'} &= \frac{1}{2}\int_0^\infty P_{nl}(r) r^2 P_{kl'}(r) dr, \end{aligned} \tag{26}$$

where $P_{nl(kl')}(r) = r R_{nl(kl')}(r)$ and $R_{nl(kl')}(r)$ are the radial parts of the HF electron wave functions in the initial (final) states.

For any l, the following expression gives the angular distribution of photoelectrons with inclusion of nondipole terms in the lowest order of photon momentum κ:

$$\frac{d\sigma_{nl}(\omega)}{d\Omega} = \frac{\sigma_{nl}(\omega)}{4\pi}\left\{1 - \frac{\beta_{nl}(\omega)}{2} P_2(\cos\theta) + \kappa\gamma_{nl}(\omega) P_1(\cos\theta) + \kappa\eta_{nl}(\omega) P_3(\cos\theta)\right\}. \tag{27}$$

For $l = 1$ one has the following expression for the dipole angular anisotropy parameters [1,10]:

$$\beta_{np}(\omega) = \frac{2}{\tilde{D}_0^2 + 2\tilde{D}_2^2}\left[\tilde{D}_2^2 - 2\tilde{D}_0\tilde{D}_2 \cos(\bar{\delta}_0 - \bar{\delta}_2)\right]. \tag{28}$$

As one sees from (19), for $l = 1$ the relation $\beta_{np}^{(\mathrm{in})}(q = 0,\omega) = -2\beta_{np}(\omega)$ is the same as for the s subshells.

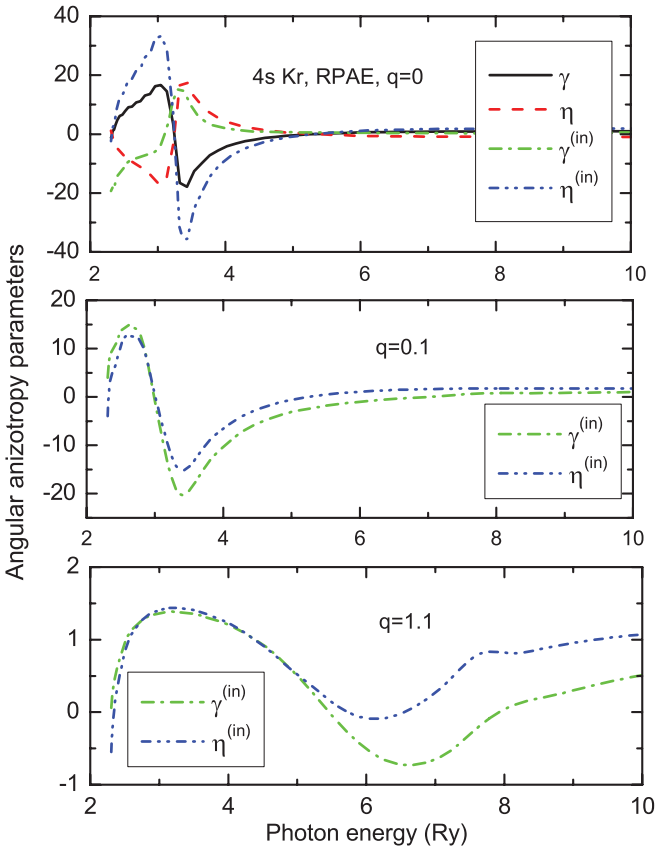

FIG. 4. (Color online) Angular anisotropy nondipole parameters of knocked-out electrons $\gamma_{ns}^{(\mathrm{in})}(\omega)$ and $\eta_{ns}^{(\mathrm{in})}(\omega)$ given by (8) and (13) at $q = 0.01$, 0.1, and 1.1, compared to similar parameters in photoionization $\gamma_{ns}(\omega)$ and $\eta_{ns}(\omega)$ (12) for the $4s$ subshell of Kr in RPAE.

The following expressions determine the nondipole angular anisotropy parameters [1] for $l = 1$:

$$\gamma_{np}(\omega) = \frac{6}{25\left[\tilde{D}_0^2 + 2\tilde{D}_2^2\right]}\{5\tilde{D}_0\tilde{Q}_1 \cos(\bar{\delta}_1 - \bar{\delta}_0) + \tilde{D}_2[9\tilde{Q}_3 \cos(\bar{\delta}_3 - \bar{\delta}_2) - \tilde{Q}_1 \cos(\bar{\delta}_1 - \bar{\delta}_2)]\}, \tag{29}$$

$$\eta_{np}(\omega) = \frac{6}{25\left[\tilde{D}_0^2 + 2\tilde{D}_2^2\right]}\{5\tilde{D}_0\tilde{Q}_3 \cos(\bar{\delta}_3 - \bar{\delta}_0) + 2\tilde{D}_2[3\tilde{Q}_1 \cos(\bar{\delta}_1 - \bar{\delta}_2) - 2\tilde{Q}_3 \cos(\bar{\delta}_3 - \bar{\delta}_2)]\}. \tag{30}$$

For the dipole angular anisotropy parameter with $l = 2$, one has the following expression [10]:

$$\beta_{nd}(\omega) = \frac{2}{5\left[2\tilde{D}_1^2 + 3\tilde{D}_3^2\right]}\left[\tilde{D}_1^2 + 6\tilde{D}_3^2 - 18\tilde{D}_1\tilde{D}_3 \cos(\bar{\delta}_1 - \bar{\delta}_3)\right]. \tag{31}$$

Note that for $l = 2$, as is seen from (22), the relation similar to $l = 0; 1$ is valid, namely, $\beta_{nd}^{(\mathrm{in})}(q = 0,\omega) = -2\beta_{nd}(\omega)$. It is quite possible that such a relation is valid for any l.

The following expressions determine the nondipole angular anisotropy parameters [1] for $l = 2$:

$$\gamma_{nd}(\omega) = \frac{6}{35\left[2\tilde{D}_1^2 + 3\tilde{D}_3^2\right]}\{7\tilde{D}_1[\tilde{Q}_2 \cos(\bar{\delta}_2 - \bar{\delta}_1) - \tilde{Q}_0 \cos(\bar{\delta}_0 - \bar{\delta}_1)] + 3\tilde{D}_3[6\tilde{Q}_4 \cos(\bar{\delta}_4 - \bar{\delta}_3) - \tilde{Q}_2 \cos(\bar{\delta}_2 - \bar{\delta}_2)]\}, \tag{32}$$

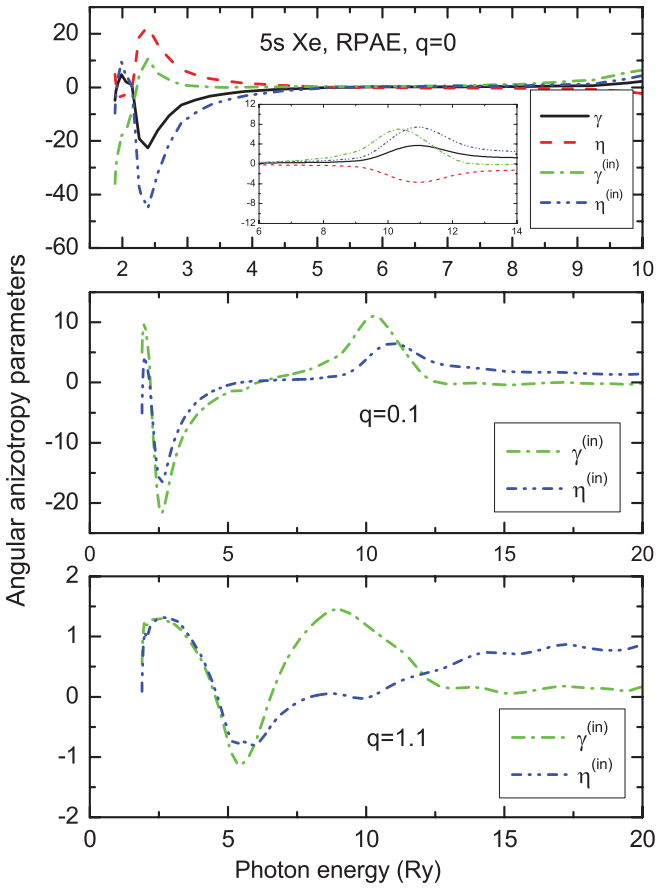

FIG. 5. (Color online) Angular anisotropy nondipole parameters of knocked-out electrons $\gamma_{ns}^{(\mathrm{in})}(\omega)$ and $\eta_{ns}^{(\mathrm{in})}(\omega)$ given by (8) and (13) at $q = 0.01$, 0.1, and 1.1, compared to similar parameters in photoionization $\gamma_{ns}(\omega)$ and $\eta_{ns}(\omega)$ (12) for the $5s$ subshell of Xe in RPAE.

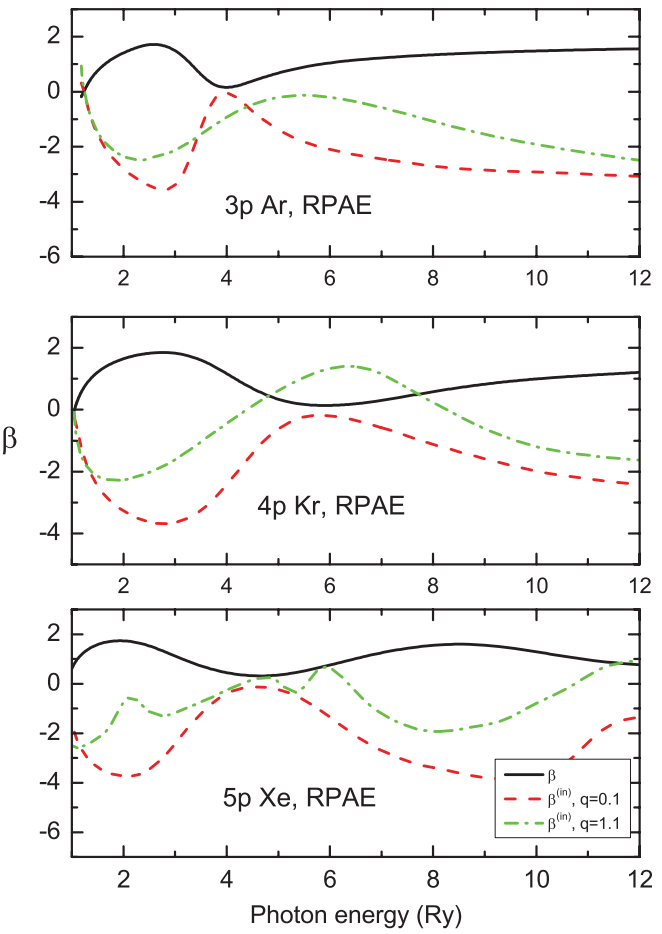

FIG. 6. (Color online) Angular anisotropy dipole parameter of knocked-out electrons $\beta_{np}^{(\mathrm{in})}(q,\omega)$ given by (15) at $q = 0.1$ and 1.1, compared to similar parameters in photoionization $\beta_{np}(\omega)$, given by (28) for the outer subshells of Ar, Kr, and Xe in RPAE.

$$\eta_{nd}(\omega) = \frac{6}{35\left[2\tilde{D}_1^2 + 3\tilde{D}_3^2\right]}\{2\tilde{D}_1[6\tilde{Q}_4\cos(\bar{\delta}_4 - \bar{\delta}_1) - \tilde{Q}_2\cos(\bar{\delta}_2 - \bar{\delta}_1)] - \tilde{D}_3[8\tilde{Q}_2\cos(\bar{\delta}_2 - \bar{\delta}_3) - 6\tilde{Q}_4\cos(\bar{\delta}_4 - \bar{\delta}_3) - 7\tilde{Q}_0\cos(\bar{\delta}_0 - \bar{\delta}_3)]\}. \quad (33)$$

Prominent analytic deviation from respective nondipole parameters for the inelastic scattering, given by (20), (21), (23), and (24) is clearly seen. Contrary to the dipole parameters, simple frequency-independent relations that connect respective nondipole parameters for photoionization and fast electron inelastic scattering do not exist.

Note that the limit $q = 0$ at $\omega \neq 0$ cannot be achieved since no energy can be transferred from the incoming electron to the projectile without momentum transfer. However, with growth of the projectile's speed, smaller and smaller q is sufficient to transfer the given energy ω.

One sees that in spite of the visibly deep similarity between photoionization and fast electron scattering, a big difference exists. Indeed, the angular distributions in photoionization and fast electron scattering are different even in the limit $q \to 0$. One can explain it by the difference between the transverse (in photoionization) and longitudinal (in fast electron scattering) photons that ionize the target atom. Analytically, it is reflected in the difference between operators causing ionization by photons and fast electrons that already include only the lowest nondipole corrections. For the photoionization, it is $(\vec{e}\cdot\vec{r}) + i(\vec{\kappa}\cdot\vec{r})(\vec{e}\cdot\vec{r})$, where $\vec{e}$ is the photon polarization operator that is orthogonal to the direction of light propagation given by the photon momentum $\vec{\kappa}$. As to fast electron scattering, it is $(\vec{q}\cdot\vec{r}) + i(\vec{q}\cdot\vec{r})(\vec{q}\cdot\vec{r})$, thus including only one angle between $\vec{q}$ and $\vec{r}$ contrary to the case of photoionization with its two angles—between $\vec{r}$, $\vec{e}$, and $\vec{\kappa}$.

Because of this difference, in photoionization the force that acts upon the outgoing electron is orthogonal to the direction of $\vec{\kappa}$ and thus of the photon beam. Therefore, the photoelectron emission is minimal along $\vec{\kappa}/\kappa$, while in inelastic electron scattering the force and maximal knocked-out electron yield is directed along $\vec{q}$.

III. CALCULATION DETAILS

In order to obtain $dF_{nl}(q,\omega)/d\Omega$ from experiment, one has to measure the yield of electrons with energy $\varepsilon = k^2/2 = \omega - I_{nl}$ emitted at a given angle θ in coincidence with the fast outgoing particle that loses energy ω and transfers to the target atom momentum $\vec{q}$. Note that according to (8), (11), and (12)

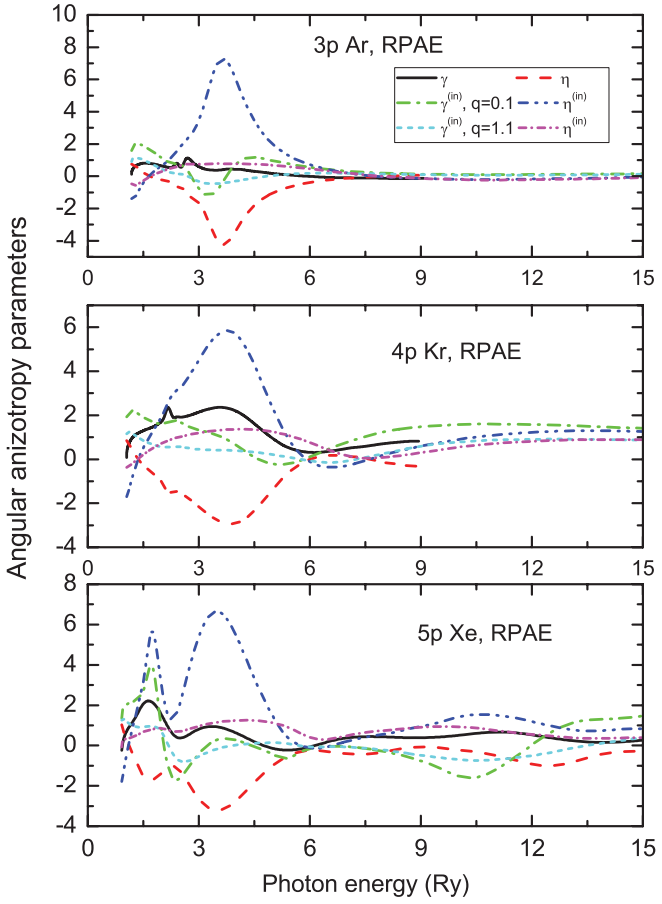

FIG. 7. (Color online) Angular anisotropy parameters of knocked-out electrons $\gamma_{np}^{(\mathrm{in})}(q,\omega)$ and $\eta_{np}^{(\mathrm{in})}(q,\omega)$ given by (15) at $q = 0.1$ and 1.1, compared to similar parameters in photoionization $\gamma_{np}(\omega)$ and $\eta_{np}(\omega)$ given by (29) and (30) for the $3p$ Ar, $4p$ Kr, and $5p$ Xe subshells in RPAE.

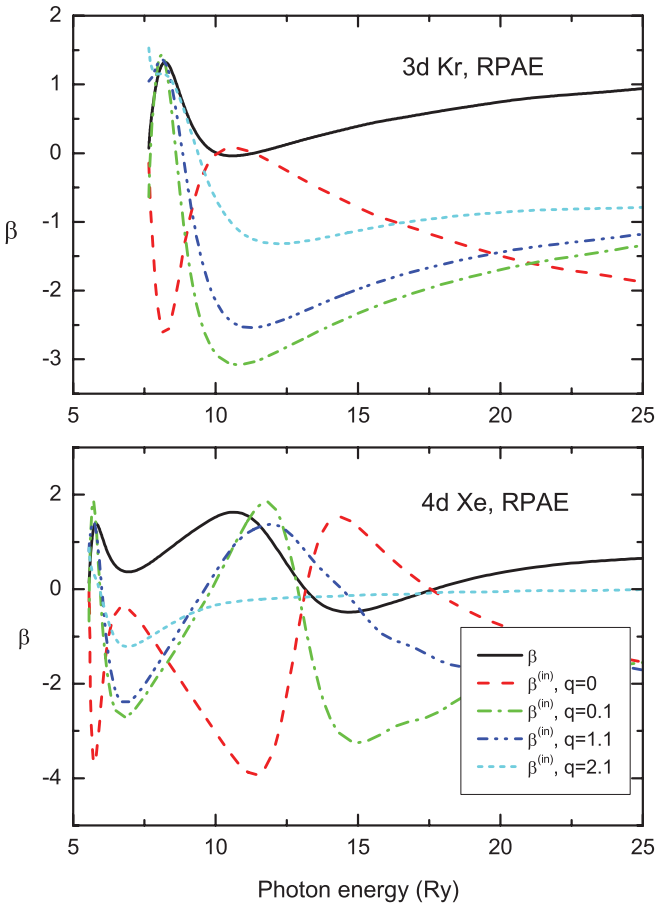

FIG. 8. (Color online) Angular anisotropy dipole parameter of knocked-out electrons $\beta_{nd}^{(\mathrm{in})}(q,\omega)$ given by (17) and (22) at $q = 0$, 0.1, 1.1 and 2.1 compared to similar parameters in photoionization $\beta_{nd}(\omega)$, given by (31) for the $3d$ Kr and $4d$ Xe subshells in RPAE.

$\beta_{n0}^{(\mathrm{in})} = -4$, which differs by sign and value from photoionization value $\beta_{ns} = 2$. As demonstrated by calculations, the differences in numerical values for nondipole parameters that characterize inelastic scattering and photoionization of p and d subshells are essential.

To calculate $dF_{nl}(q,\omega)/d\Omega$ we have used the numeric procedures described at length in Ref. [21]. We perform calculations in the frame of Hartree-Fock and RPAE approximations. As concrete objects, we choose outer np^2 and subvalent ns^2 subshells of Ar, Kr, and Xe. The nondipole parameter $\zeta_{nd}^{(\mathrm{in})}$ was calculated for $3d$ Kr and $4d$ Xe, using the expression that follows from (17):

$$\zeta_{nd}^{(\mathrm{in})} = \frac{90}{49qW_2}\left[20\tilde{G}_{22}^2 + \tilde{G}_{42}(98\tilde{G}_{02}\cos(\bar{\delta}_0 - \bar{\delta}_4) - 100\tilde{G}_{22}\cos(\bar{\delta}_2 - \bar{\delta}_4) + 27\tilde{G}_{42})\right]. \quad (34)$$

We perform computations using Eqs. (5)–(9), (11), (13), and (15)–(18) in HF and RPAE, for $q = 0.0, 0.1$, 1.1, and 2.1. The energies up to 20–25 Ry for outgoing electrons are considered. Note that we present the point $q = 2.1$ only for some orientation. Indeed, for not small enough q values the formulas presented and discussed in this paper are incorrect, since with the growth of q the values $L', L'' > 2$ become increasingly important.

Most prominent are the nondipole corrections at so-called magic angle θ_m, for which holds the relation $P_2(\cos\theta_m) = 0$. This is why we present the differential in emission angle GOSs $dF_{nl}(q,\omega)/d\Omega$ at the magic angle θ_m and at $q = 0.0; 0.1; 1.1; 2.1$. Results are obtained also for dipole and nondipole angular anisotropy parameters. Figures 1–11 present all data.

The lowest value of q corresponds to the photoionization limit, since $qR \ll 1$, and in the considered frequency range $\omega/c < 0.05 < q_{\min} = 0.1$. The last inequality shows that we consider the nondipole corrections to the GOSs that are much bigger than the nondipole corrections to photoionization.

IV. CALCULATION RESULTS

The results demonstrate that the GOSs and angular anisotropy parameters are complex and informative functions with a number of prominent variations. All calculated characteristics demonstrate strong influence of the electron correlations for p, s, and d electrons. They depend strongly upon the outgoing electron energy and the linear momentum q transferred to an atom in the fast electron inelastic scattering.

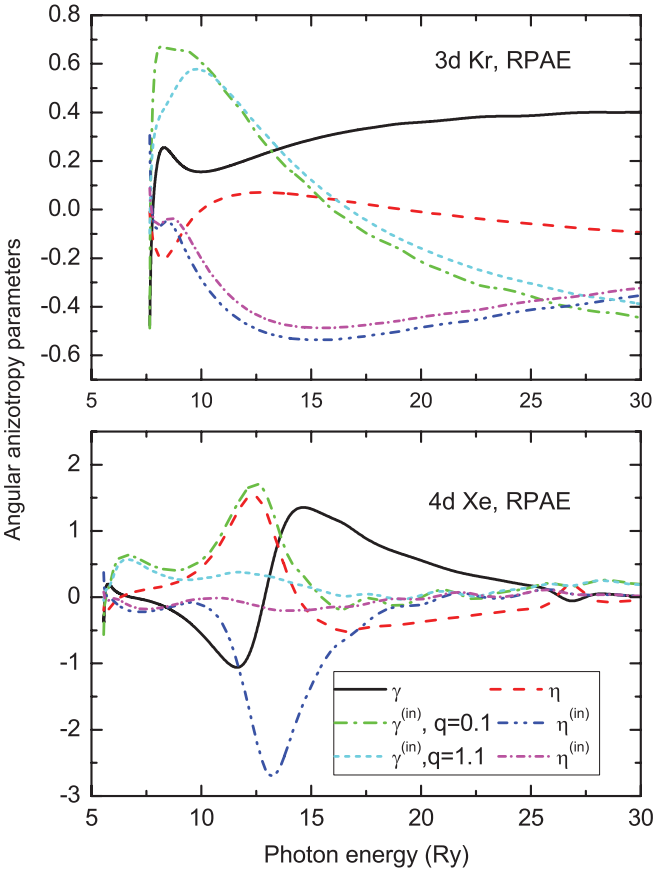

FIG. 9. (Color online) Angular anisotropy nondipole parameters of knocked-out electrons $\gamma_{nd}^{(\mathrm{in})}(q,\omega)$ and $\eta_{nd}^{(\mathrm{in})}(q,\omega)$ given by (17) at $q = 0.1$ and 1.1, compared to similar parameters in photoionization $\gamma_{np}(\omega)$ and $\eta_{np}(\omega)$, given by (32) and (33) for the $3d$ Kr and $4d$ Xe subshells in RPAE.

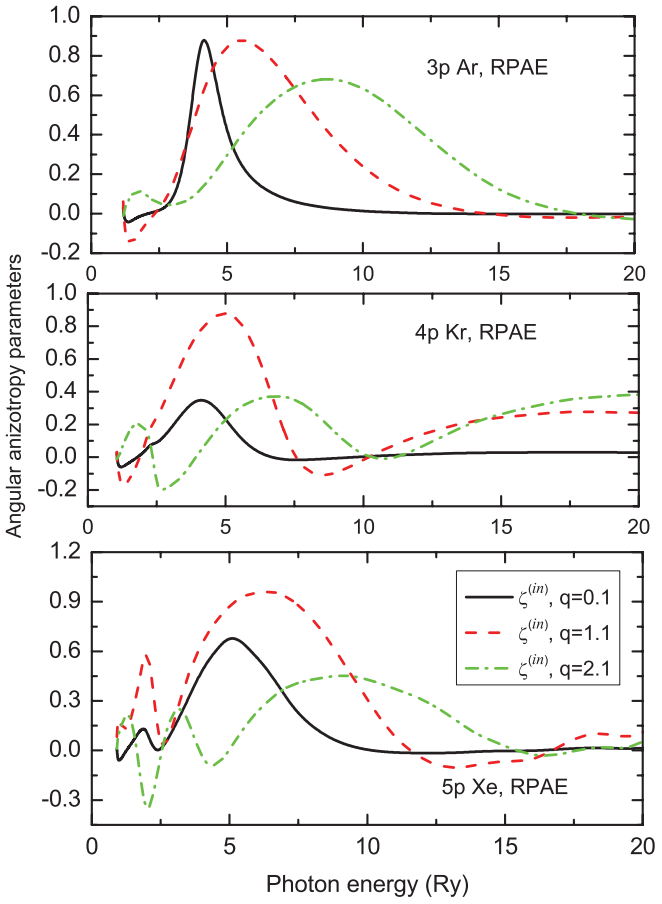

FIG. 10. (Color online) Angular anisotropy nondipole parameter—coefficient of the fourth Legendre polynomial in the angular distribution of the knocked-out electrons $\zeta_{np}^{(\mathrm{in})}(q,\omega)$, calculated using (15). The results are presented for the $3p$ Ar, $4p$ Kr, and $5p$ Xe subshells at $q = 0.1$, 1.1, and 2.1.

Electron correlations strongly affect the results. Figures 2, 3, and 5 have an overlap with that presented in Ref. [11]. They are different in value, since in this paper we use a much improved computing code.

Figures 1 and 2 present differential GOSs given by (15) and (8) at the magic angle $\theta_m \cong 54.7^\circ$ for outer np and subvalent ns subshells of Ar, Kr, and Xe at $q = 0.1$, 1.1, and 2.1 in HF and RPAE. At small q the GOSs are similar to the photoionization cross section. For p subshells with growth of q the maximum decreases in magnitude and shifts to higher ω. For $q =$ 2.1 there is no trace of any similarity with photoionization. The situation for the s subshell is different, since here the differential GOSs with an increase of q at first grow and only then start rapidly to decrease. Note a particularly strong effect of RPAE correlations near threshold.

The insertion in Fig. 1 for $5p$ Xe shows the prominent effect played by the action of $4d$ giant resonance upon $5p$ GOS. For big q, $q = 2.1$, the maximum exists at the same energy already in HF, and the action of $4d$ adds only a small shoulder.

Figures 3–5 collect values for the nondipole angular anisotropy parameters of knocked-out electrons $\gamma_{ns}^{(\mathrm{in})}(\omega)$ and $\eta_{ns}^{(\mathrm{in})}(\omega)$ given by (7) and (14) at $q = 0.01$, 0.1, and 1.1, compared to similar parameters in the photoionization $\gamma_{ns}(\omega)$ and $\eta_{ns}(\omega)$ (11) for the subvalent ns subshell of Ar, Kr, and Xe in RPAE. For $q = 0$ the relation $\eta_{ns}^{(\mathrm{in})}(\omega) = 2\gamma_{n0}(\omega)$ is valid. As to $\gamma_{ns}^{(\mathrm{in})}(\omega)$, it is of a different sign and three to four times bigger than $\eta_{ns}(\omega)$. This means that even in the limit $q = 0$ the nondipole parameters for photoionization and for fast electron inelastic scattering are essentially different. Qualitatively, the parameters at $q = 0.1$ look similar to those at $q = 0$, but smaller. With an increase of q, the variation becomes broader and shifts to the higher ω side. Note that an approximate relation proved to be valid between $\gamma_{ns}^{(\mathrm{in})}(\omega)$ and $\eta_{ns}^{(\mathrm{in})}(\omega)$.

Figure 6 presents the dipole angular anisotropy parameter of the knocked-out electrons $\beta_{np}^{(\mathrm{in})}(q,\omega)$ given by (15) at $q = 0.1$ and 1.1, compared to a similar parameter in the photoionization $\beta_{np}(\omega)$, given by (28), for the outer subshells of Ar, Kr, and Xe in RPAE. It is seen that for $q = 0.1$ the relation, which is precisely correct at $q = 0, \beta_{np}^{(\mathrm{in})}(q = 0,\omega) = -2\beta_{np}(\omega)$ is approximately valid, while it is violated for bigger q. It looks like the inequality $-4 \leqslant \beta_{nl}^{(\mathrm{in})}(q,\omega) \leqslant 2$ holds. Maximum for $\beta_{np}(\omega)$ and minima for $\beta_{np}^{(\mathrm{in})}(q,\omega)$ in Xe in the ω region around 8–10 Ry are consequences of the effect of the $4d$ giant resonance.

Figure 7 depicts the angular anisotropy nondipole parameters of knocked-out electrons $\gamma_{np}^{(\mathrm{in})}(q,\omega)$ and $\eta_{np}^{(\mathrm{in})}(q,\omega)$ given by (15) at $q = 0.1$ and 1.1, compared to similar parameters

in the photoionization $\gamma_{np}(\omega)$ and $\eta_{np}(\omega)$ given by (29) and (30) for $3p$ Ar, $4p$ Kr, and $5p$ Xe subshells in RPAE. As is already seen from the analytic expressions, the difference between photoionization values and that for the fast electron scattering is essential even in the limit $q = 0$. The nondipole parameters are complex and thus rather informative functions of ω at both $q$values.

Figure 8 represents the angular anisotropy dipole parameter of knocked-out electrons $\beta_{nd}^{(\mathrm{in})}(q,\omega)$ given by (17) and (22) at $q = 0.1$, 1.1, and 2.1, compared to similar parameters in the photoionization $\beta_{nd}(\omega)$, given by (31) for $3d$ Kr and $4d$ Xe subshells in RPAE. Note that the relation $\beta_{nd}^{(\mathrm{in})}(q = 0,\omega) = -2\beta_{nd}(\omega)$ is fulfilled. Prominent changes of $\beta_{nd}^{(\mathrm{in})}(q,\omega)$ take place with the weakening of variations, while q increases.

Figure 9 shows the angular anisotropy nondipole parameters of knocked-out electrons $\gamma_{nd}^{(\mathrm{in})}(q,\omega)$ and $\eta_{nd}^{(\mathrm{in})}(q,\omega)$ given by (17) at $q = 0.1$ and 1.1, compared to similar parameters in photoionization $\gamma_{nd}(\omega)$ and $\eta_{nd}(\omega)$, determined by (32) and (33) for $3d$ Kr and $4d$ Xe subshells in RPAE. The difference between parameters for photoionization and fast electron scattering is quite large. Note that the parameters, as it should be, are smaller than the data for respective $p$subshells since the radii $3d$ Kr and $4d$ Xe are smaller than those of $4p$ Kr and $5p$ Xe, respectively.

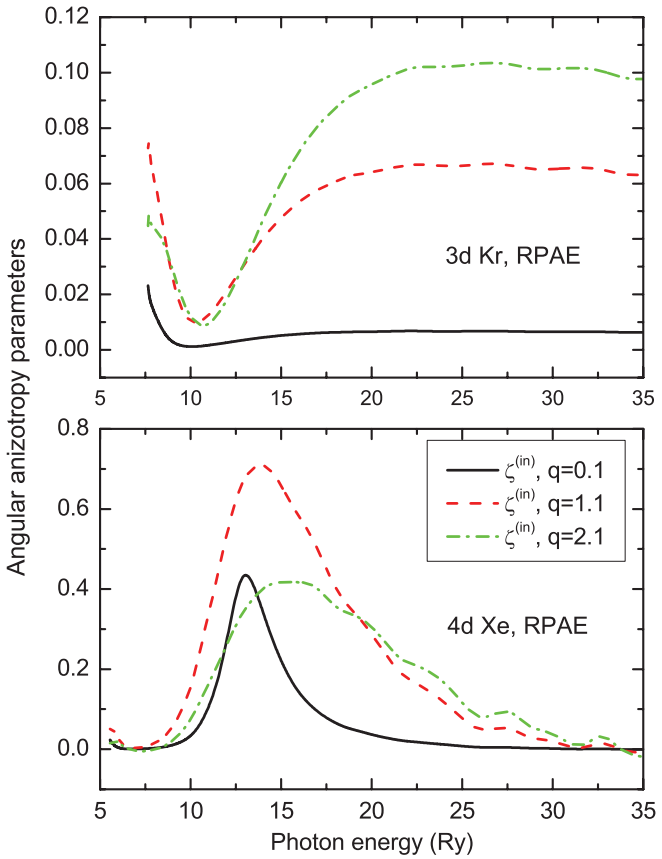

FIG. 11. (Color online) Anisotropy nondipole parameter $\zeta_{nd}^{(\mathrm{in})}(q,\omega)$—coefficient of the fourth Legendre polynomial in the angular distribution of the knocked-out electrons $\zeta_{nl}^{(\mathrm{in})}(q,\omega)$, calculated at $q = 0.1$, 1.1 and 2.1 using (17). The results are presented for the outer and nd subshells of the Ar, Kr, and Xe subshells.

Figure 10 demonstrates the last angular anisotropy nondipole parameter, namely, the coefficient of the fourth Legendre polynomial in the angular distribution of the knocked-out electrons $\zeta_{np}^{(\mathrm{in})}(q,\omega)$, calculated using (15). The results are presented for the $3p$ Ar, $4p$ Kr, and $5p$ Xe subshells at $q = 0.1$, 1.1, and 2.1. This parameter does not have a calculated photoionization analog. The absolute value is much smaller than other nondipole parameters for the same subshells.

Figure 11 gives the data on the angular anisotropy nondipole parameter $\zeta_{nd}^{(\mathrm{in})}(q,\omega)$—coefficient of the fourth Legendre polynomial in the angular distribution of the knocked-out electrons, calculated at $q = 0.1$,1.1 and $q = 2.1$ using (17). The results are presented for $3d$ Kr and $4d$ Xe subshells. These results are much smaller than in Fig. 10 since the respective radii are for the $3d$ and $4d$ subshells, smaller than for $4p$ and $5p$, respectively.

V. CONCLUDING REMARKS

It is not a surprise that GOSs and angular anisotropy parameters depend upon q and ω. What is indeed a surprise is the big difference between the angular anisotropy parameters for fast electron scattering and their respective photoionization values. Already from photoionization studies, we know that they are strongly affected by atomic electron correlations. Here we saw that fast electron scattering also gives information on transferred momentum dependences and their interplay with electron correlations.

The biggest unexpected feature of the angular anisotropy for the inelastic scattering is that even in the $q = 0$ limit they do not coincide with respective photoionization values, and they are not connected by a simple relation similar to that between the photoionization cross section and GOSs. This is a result of different operators for photoionization and fast electron scattering as is discussed at the very end of Sec. III.

We expect that this paper will stimulate experimental efforts in the not too simple but potentially rather informative studies of the differential cross section of secondary electrons knocked out off a target atom in fast electron-atom collisions. We understand that such studies require coincidence experiments, in which simultaneously the transferred by fast electron energy and momentum are fixed, as well as the momentum of the secondary electron.

In particular, the $q \to 0$ limit deserves special attention. It is already seen that the dipole angular anisotropy parameters are different by sign and value. The nondipole parameters, in their turn, deviate even qualitatively from their respective photoionization values. It is amazing that in the nonrelativistic domain of energies inessential at first glance difference between a virtual and a real photon leads to such prominent consequences.

The information that could come from studies of angular distribution of secondary electrons at small q is of great interest and value. Thus, the experimental studies suggested here are desirable.

ACKNOWLEDGMENTS

The authors are grateful for the financial assistance via the Israeli-Russian Grant No. RFBR-MSTI 11-02-92484.

[1] M. Ya. Amusia, A. S. Baltenkov, L. V. Chernysheva, Z. Felfli, and A. Z. Msezane, Phys. Rev. A **63**, 052506 (2001).
[2] J. W. Cooper, Phys. Rev. A **42**, 6942 (1990); **45**, 3362 (1992); **47**, 1841 (1993).
[3] A. Bechler and R. H. Pratt, Phys. Rev. A **42**, 6400 (1990).
[4] B. Krassig, M. Jung, D. S. Gemmell, E. P. Kanter, T. LeBrun, S. H. Southworth, and L. Young, Phys. Rev. Lett. **175**, 4736 (1995).
[5] E. P. Kanter, B. Krassig, S. H. Southworth, R. Guillemin, O. D. Hemmers, W. Lindle, R. Wehlitz, M. Ya. Amusia, L. V. Chernysheva, and N. L. S. Martin, Phys. Rev. A **68**, 012714 (2003).
[6] O. Hemmers, R. Guillemin, E. P. Kanter, B. Krassig, D. Lindle, S. H. Southworth, R. Wehlitz, J. Baker, A. Hudson, M. Lotrakul, D. Rolles, W. C. Stolte, I. C. Tran, A. Wolska, S. W. Yu, M. Ya. Amusia, K. T. Cheng, L. V. Chernysheva, W. R. Johnson, and S. T. Manson, Phys. Rev. Lett. **91**, 053002 (2003).
[7] A. Kivimäki, U. Hergenhahn, B. Kempgens, R. Hentges, M. N. Piancastelli, K. Maier, A. Ruedel, J. J. Tulkki, and A. M. Bradshaw, Phys. Rev. A **63**, 012716 (2000).
[8] T. M. El-Sherbini and M. J. Van der Wiel, Physica **62**, 119 (1972).
[9] M. Ya. Amusia and N. A. Cherepkov, Case Stud. At. Phys. **5**, 47 (1975).
[10] M. Ya. Amusia, *Atomic Photoeffect* (Plenum Press, New York, 1990).
[11] M. Ya. Amusia, L. V. Chernysheva, and E. Z. Liverts, JETP Lett. **94**, 431 (2011).
[12] M. Ya. Amusia, L. V. Chernysheva, Z. Felfli, and A. Z. Msezane, Phys. Rev. A **67**, 022703 (2003).
[13] Zhu Lin-Fan, Cheng Hua-Dong, Yuan Zhen-Sheng, Liu Xiao-Jing, Sun Jian-Min, and Xu Ke-Zun, Phys. Rev. A **73**, 042703, (2006).
[14] H. Ehrhardt, K. H. Hesselbacher, K. Jung, E. Schubert, and K. Willmann, J. Phys. B **7**, 69 (1974).
[15] A. Lahmam-Bennani, H. F. Wellenstein, A. Duguet, and M. Rouault, J. Phys. B **16**, 121 (1983).
[16] A. Prideaux and D. H. Madison, Phys. Rev. A **67**, 052710 (2003).
[17] M. Stevenson, G. J. Leighton, A. Crowe, K. Bartschat, and O. K. Vorov, J. Phys. B **38**, 433 (2005).
[18] M. Inokuti, Rev. Mod. Phys. **43**, 297 (1971).
[19] L. D. Landau and E. M. Lifshitz, *Quantum Mechanics. Non-Relativistic Theory* (Pergamon, Oxford, 1965).
[20] M. Ya. Amusia, Radiat. Phys. Chem. **70**, 237 (2004).
[21] M. Ya. Amusia and L. V. Chernysheva, *Computation of Atomic Processes* (Institute of Physics, Bristol, 1997).
[22] See [http://wolfram.com].